

Non-hydrodynamic collective modes in liquid metals and alloys

T. Bryk^{1,2,a}

¹ Institute for Condensed Matter Physics, National Academy of Sciences of Ukraine,
1 Svientsitskii Street, UA-79011 Lviv, Ukraine

² Institute of Applied Mathematics and Fundamental Sciences, National Polytechnic
University of Lviv, UA-79013 Lviv, Ukraine

Received 01 December 2010 / Received in final form 13 April 2011
Published online 30 May 2011

Abstract. A short review of analytical and numerical results, obtained for collective dynamics in liquid metals and alloys within a theoretical approach of Generalized Collective Modes (GCM) is presented. The GCM approach permits to represent dynamic structure factors in wide ranges of wave numbers and frequencies as a sum of contributions from hydrodynamic and non-hydrodynamic processes. The origin of collective modes that make important contributions to dynamic structure factors beyond the hydrodynamic regime in liquid metals and alloys is discussed.

1 Introduction

Microscopic collective dynamics in topologically disordered systems is one of very sophisticated and still unsolved problems of statistical mechanics. Only on macroscopic spatial and time scales when disordered systems can be treated as continuum with local conservation laws one can obtain analytical expressions for hydrodynamic density-density time correlation function $F_{nn}(k, t)$ and their time Fourier transform called dynamic structure factor $S(k, \omega)$, where k and ω denote wave number and frequency, respectively [1–3]. Dynamic structure factors can be measured for a wide range of wave numbers in inelastic X-ray scattering (IXS) or inelastic neutron scattering (INS) experiments thus giving very precious information on collective dynamics in liquids on different spatial and time scales: from hydrodynamic to molecular-scale regime.

In hydrodynamic regime the $S(k, \omega)$ has a three-peak shape: Rayleigh peak centered at zero frequency due to relaxing non-propagating processes in liquid, and two Brillouin side peaks centered at frequencies $\pm\omega_s$ due to propagating long-wavelength longitudinal excitations.

The only propagating hydrodynamic modes in collective dynamics of liquids on macroscopic scales are the longitudinal long-wavelength acoustic excitations with

^a e-mail: bryk@icmp.lviv.ua

linear dispersion law

$$\omega_s(k) = c_s k$$

and quadratic in k damping

$$\sigma_s(k) = \Gamma k^2,$$

where c_s is adiabatic speed of sound and Γ is sound damping coefficient. Long-wavelength transverse acoustic excitations in liquids do not exist in hydrodynamic regime - they cannot be supported by liquids on macroscopic distances.

Hydrodynamic solutions for relaxation processes in liquids have a common feature: their relaxation times increase in the long-wavelength limit as

$$\tau_i(k) = \frac{1}{D_i k^2},$$

where D_i is usually some coefficient connected with corresponding transport coefficient, like D_{12} being mutual diffusivity or $D_T = \lambda/nC_p$ - thermal diffusivity defined via thermal conductivity λ , numerical density n and specific heat at constant pressure C_p .

Hydrodynamic time correlation functions [1, 3] are represented as a separable sum over a few terms, each of which is associated with so-called *collective mode*. The number of hydrodynamic collective modes is defined by the number of conserved quantities in the system because hydrodynamic set of equations represents in fact local conservation laws. For pure liquids the density-density time correlation functions in hydrodynamic regime contain three terms

$$\begin{aligned} F_{nn}(k, t)/S(k) = \langle n(k, t)n^*(k, t=0) \rangle / S(k) &= \left(1 - \frac{1}{\gamma}\right) e^{-D_T k^2} + \frac{1}{\gamma} e^{-\Gamma k^2} \cos[c_s k t] \\ &+ \frac{[\Gamma + (\gamma - 1)D_T]k}{\gamma c_s} e^{-\Gamma k^2} \sin[c_s k t]. \end{aligned} \quad (1)$$

Here γ is the ratio of specific heats and $S(k)$ - static structure factor. First term in (1) comes from a relaxing mode connected with thermal diffusivity, while two other terms represent damped oscillations and correspond to propagating acoustic modes.

For transverse dynamics there exists the only conserved quantity which is the transverse component of total momentum, and this results in a single-exponential form for hydrodynamic transverse current autocorrelation function

$$C^T(k, t) = \langle J^T(k, t)J^{T*}(k, t=0) \rangle = m k_B T e^{-\eta k^2 t / \rho}, \quad (2)$$

that represents the only hydrodynamic relaxing mode connected with shear viscosity η . In (2) $\rho = mN/V$ is the mass-density of the system composed of N particles in volume V , and k_B and T are Boltzmann constant and temperature, respectively.

General feature for all the contributions from hydrodynamic modes to $F_{nn}(k, t)$ is their exponential decay, which however becomes extremely small in hydrodynamic limit $k \rightarrow 0$ because of the presence of k^2 in exponentials in (1) and (2). And this fact clearly reflects the essence of hydrodynamics: it describes only most slow collective processes in liquids, that survive on macroscopic distances.

2 Concept of non-hydrodynamic collective modes

Several schemes of generalization of hydrodynamic theory were proposed in order to describe microscopic dynamics in liquids on molecular spatial and time scales [1, 2, 4]. Most of them are based on formalism of memory functions [1] and use some assumptions in order to represent time (or frequency) dependence of the memory functions (or their Fourier transforms) leading in the end to sophisticated expressions for dynamic structure factors $S(k, \omega)$.

However, one of the schemes of generalized hydrodynamics [5, 6] permits similar and quite simple as in hydrodynamic theory representation of time correlation functions (and corresponding dynamic structure factors) in liquids via a separable sum of contributions from collective modes in a wide region of wave numbers. In general the expression for time correlation functions reads as follows:

$$F_{nn}(k, t) = \sum_i^{N_v} G_{nn}^i(k) e^{-z_i(k)t}, \quad (3)$$

where the sum is over N_v mode contributions, and $z_i(k)$ and weight coefficients $G_{nn}^i(k)$ are in general case complex functions of wave number k . Two features permit to separate in this expression contributions from hydrodynamic modes. In the long-wavelength limit the contributions from hydrodynamic processes have the weight coefficients $G_{nn}^i(k)$ tending to non-zero constants, and $z_i(k)$ tending to hydrodynamic expressions like:

$$z_s^\pm(k) \xrightarrow{k \rightarrow 0} \sigma_s(k) \pm i\omega_s(k) \equiv \frac{1}{2}[D_L + (\gamma - 1)D_T]k^2 \pm ic_s k \quad (4)$$

for longitudinal acoustic excitations and

$$Re[z_i(k)] \xrightarrow{k \rightarrow 0} D_i k^2 \quad (5)$$

for all the hydrodynamic processes. In (4) D_L denotes kinematic viscosity.

In contrast to hydrodynamic collective modes the other contributions in Eq. (3) have vanishing in the long-wavelength limit weight coefficients $G_{nn}^i(k)$ and tending to some non-zero constants values of $z_i(k)$. From the point of view of exponential time decay in Eq. (3) this means, that the collective processes with non-vanishing values $z_i(k)$ in $k \rightarrow 0$ limit have finite lifetime and therefore cannot survive on macroscopic distances. Actually this is the main feature of non-hydrodynamic processes: they can be neglected on macroscopic time and spatial scales, however on microscopic scales they contribute to the observable intensities in IXS and INS experiments.

A theoretical method that permits a consistent description of hydrodynamic and non-hydrodynamic collective processes in liquids and represents time correlation functions and corresponding spectral functions via separable sum of contributions coming from *dynamic eigenmodes* that can exist in the system on different spatial and time scales is known as the approach of Generalized Collective Modes (GCM) [7, 8]. Theoretical basis of the GCM approach was very well described in a review [6]. Therefore here we will give only a short description of the GCM methodology and its application in studies of non-hydrodynamic collective modes in liquid metals and alloys.

The GCM approach is based on eigenvalue problem for the generalized Langevin equation in matrix form, that is generated on a chosen *extended* set of N_v dynamic variables. Propagating dynamic eigenmodes are represented by complex-conjugated pairs of eigenvalues, while purely real eigenvalues describe non-propagating relaxing processes. Corresponding eigenvectors associated with some $z_i(k)$ eigenvalue define its weight coefficients $G^i(k)$ in all time correlation functions of interest [6].

Let us consider here a simple generalized model for longitudinal dynamics of pure liquids. For pure liquids the hydrodynamic set of variables for description of longitudinal dynamics consists of three conserved dynamic variables [1, 9]:

$$\mathbf{A}^{(3hyd)}(k, t) = \{n(k, t), J^L(k, t), e(k, t)\}, \quad (6)$$

where the k -th spatial-Fourier components of number density $n(k, t)$ of the system, composed of N classical particles with instantaneous positions $\mathbf{r}_i(t)$ and velocities $\mathbf{v}_i(t)$, is defined as follows

$$n(k, t) = \frac{1}{\sqrt{N}} \sum_{j=1}^N e^{i\mathbf{k}\mathbf{r}_j(t)}. \quad (7)$$

The other hydrodynamic variables in (6) are the Fourier-components of longitudinal component of mass-current density

$$J^L(k, t) = \frac{1}{\sqrt{N}} \frac{m}{k} \sum_{j=1}^N \mathbf{k}\mathbf{v}_j e^{i\mathbf{k}\mathbf{r}_j(t)} \quad (8)$$

and energy density

$$e(k, t) = \frac{1}{\sqrt{N}} \sum_{j=1}^N \varepsilon_j e^{i\mathbf{k}\mathbf{r}_j(t)}, \quad (9)$$

where ε_j is the single-particle energy of j -th particle. In order to account for non-hydrodynamic processes in dynamics of pure liquids within the GCM approach we apply for solving the generalized Langevin equation the simplest extended set of five dynamic variables

$$\mathbf{A}^{(5)}(k, t) = \{n(k, t), J^L(k, t), e(k, t), \dot{J}^L(k, t), \dot{e}(k, t)\}, \quad (10)$$

where extended dynamic variables represent the first time derivatives of the longitudinal component of mass-current and energy density. Since the static correlations between a dynamic variable and its first time derivative due to symmetry reasons for equilibrium classical systems is zero [1] the extended set of dynamic variables $\mathbf{A}^{(5)}(k, t)$ contains processes, that are orthogonal to the hydrodynamic ones. Hence the extended dynamic variables are aimed to describe correctly short-time fluctuations. The chosen set of five dynamical variables is used for construction of a 5×5 generalized hydrodynamic matrix $\mathbf{T}^{(5)}(k)$ defined [6] as

$$\mathbf{T}^{(5)}(k) = \mathbf{F}(k, t = 0) \tilde{\mathbf{F}}^{-1}(k, z = 0),$$

where 5×5 matrices $\mathbf{F}(k, t = 0)$ and $\tilde{\mathbf{F}}^{-1}(k, z = 0)$ are the matrix of static correlation functions and Laplace-transformed matrix of time correlation functions taken in Markovian approximation. The eigenvalues of $\mathbf{T}^{(5)}(k)$ define the spectrum of collective propagating and relaxing eigenmodes in the system, two of which in the long-wavelength limit have to correspond to non-hydrodynamic processes. Analytical solution for the extended five-variable dynamic model $\mathbf{A}^{(5)}$ in hydrodynamic regime was obtained in Ref. [10]. Therefore here we will show only results for non-hydrodynamic collective modes.

Five eigenvalues of the dynamic model $\mathbf{A}^{(5)}$ in the long-wavelength limit contain three hydrodynamic modes: a pair of complex-conjugated eigenvalues (4) that correspond to acoustic excitations, and one relaxing hydrodynamic mode connected with thermal diffusivity:

$$d_1(k) \equiv d_{th}(k) \equiv \text{Re}[z_{th}(k)] = D_T k^2. \quad (11)$$

It is convenient to distinguish purely real eigenvalues and complex-conjugated pairs, and henceforth we will denote the purely real eigenvalues as $d_i(k)$. Two non-hydrodynamic purely real eigenvalues were obtained in [10] in the long-wavelength limit:

$$d_2(k) = d_2^0 - D_L k^2 + (\gamma - 1)\Delta k^2, \quad (12)$$

$$d_3(k) = d_3^0 - \gamma D_T k^2 - (\gamma - 1)\Delta k^2, \quad (13)$$

where the following notations were introduced:

$$d_2^0 = \frac{c_\infty^2 - c_s^2}{D_L}, \quad (14)$$

$$d_3^0 = \frac{c_V}{m\lambda} \left(G^h - \frac{(\gamma - 1)}{\kappa_T} \right), \quad (15)$$

and

$$\Delta = \frac{d_2^0 d_3^0}{d_3^0 - d_2^0} \frac{D_T}{D_L c_s^2} (D_T - D_L)^2. \quad (16)$$

In these expressions c_∞ , c_V , G^h and κ_T are the high-frequency speed of sound, specific heat at constant volume, heat rigidity [11] and isothermal compressibility, respectively. One can see, that both non-hydrodynamic relaxing modes tend in the limit $k \rightarrow 0$ to some non-zero values, that means finite lifetimes on macroscopic scales.

If one neglected the coupling between thermal and density fluctuations, i.e. put in $\gamma = 1$ that is quite justified for the case of metals, it is easy to estimate the origin of both non-hydrodynamic relaxing processes. The relaxing mode $d_2(k)$ tends to a constant d_2^0 , that is inversely proportional to kinematic viscosity D_L . This means, that approaching the glass transition this non-hydrodynamic relaxation will have almost infinite relaxation time, that is one of the features of structural alpha-relaxation. Besides, the factor $c_\infty^2 - c_s^2$ is associated in the literature with the “strength” of structural relaxation [12]. These two facts imply that the collective mode $d_2(k)$ reflects the non-hydrodynamic structural relaxation on macroscopic scales.

Another non-hydrodynamic relaxing mode $d_3(k)$ is purely of thermal origin. It will be shown below, that this non-hydrodynamic heat relaxing process is connected with emergence of heat waves in liquids on microscopic scales.

Analytical solutions for non-hydrodynamic modes usually can be obtained only in the long-wavelength limit. However, numerical solutions for the five-variable dynamic model $\mathbf{A}^{(5)}$ can be calculated in the whole range of wave numbers accessible from molecular dynamic simulations. In Fig. 1 the spectrum of complex and purely real dynamic eigenvalues is shown for the case of liquid Ca near the melting point. Simulations for Ca and other liquid alkaline earth metals reported in this paper were performed on model systems of 2000 particles interacting via effective pair potentials taken from Ref. [13]. It follows from Fig. 1 that for $k < 0.2 \text{ \AA}^{-1}$ one observes five eigenvalues in good agreement with analytical results. One can see, that the mode $d_2(k)$ shown by “star” symbols behaves approximately as

$$d_2(k) \approx d_2^0 - D_L k^2,$$

and for larger wave numbers it becomes the slowest relaxation process in the system on nanoscales, while in hydrodynamic regime the thermodiffusive hydrodynamic mode $d_1(k)$ behaves in agreement with Eq. (5) and completely defines the central peak of dynamic structure factor $S(k, \omega)$. Different behaviour of $d_1(k)$ and $d_2(k)$ and their cross section around $k \approx 0.25 \text{ \AA}^{-1}$ permit to estimate the approximate width

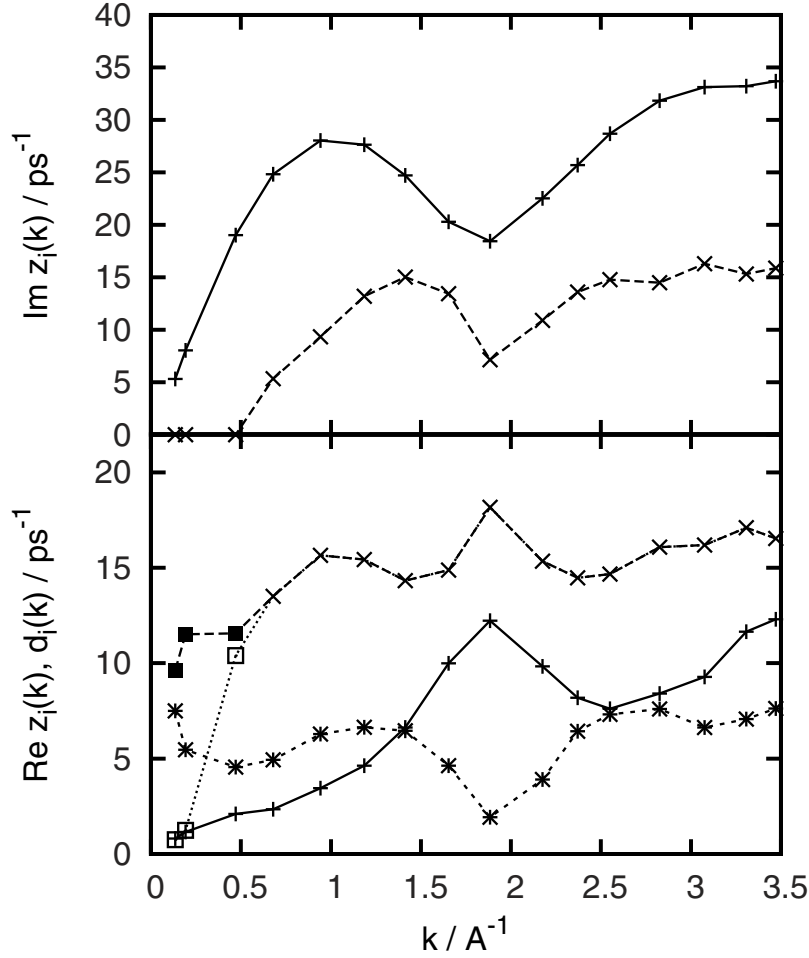


Fig. 1. Numerical solutions of the five-variable dynamic model $\mathbf{A}^{(5)}$ for liquid Ca at melting point. Line-connected symbols “plus” and “cross” correspond respectively to acoustic collective excitations and non-hydrodynamic heat waves. Open and closed boxes represent hydrodynamic and non-hydrodynamic heat relaxing modes, and symbols “star” show wave-number dependence of non-hydrodynamic structural relaxation.

of hydrodynamic regime k_{hd} [14]. For wave numbers $k > k_{hd}$ there is strong effect of non-hydrodynamic modes on collective dynamics in liquids. Effect of interaction of structural relaxation with acoustic excitations will be explained in next Section.

3 Non-hydrodynamic collective processes in liquid metals and alloys

3.1 Structural relaxation

It is obvious, that atomistic structure of matter is completely ignored in continuum approach, therefore any collective processes that emerge due to structural redistribution in disordered systems cannot be described by hydrodynamic modes. In Sec. 2 we have shown, how one of the relaxing non-hydrodynamic modes can be associated with

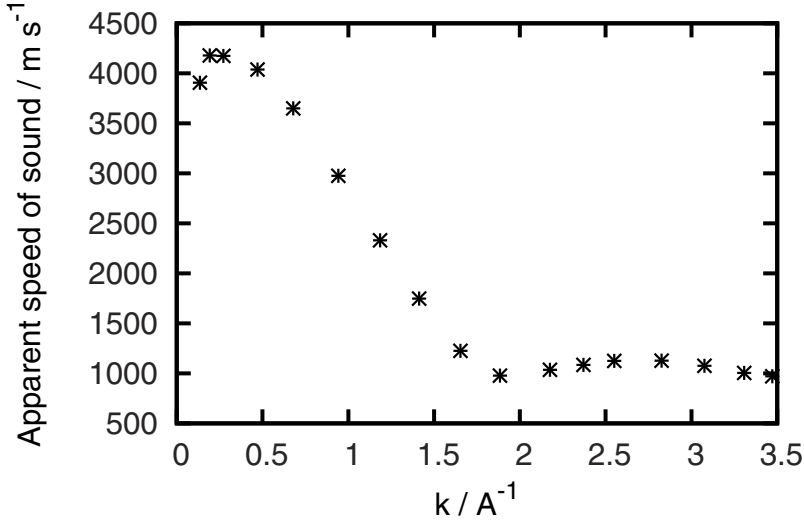


Fig. 2. Apparent speed of sound for liquid Ca at melting point.

structural relaxation. For wave numbers in the region of first sharp diffraction peak (FSDP) of static structure factor $S(k \approx k_{FSDP})$ the structural relaxation almost completely is responsible for relaxation of density-density time correlation functions. It was shown in [15, 16], that for wave numbers $k \approx k_{FSDP}$ the shape of density-density time correlation function can be analytically reproduced by a simplified single-variable dynamic model

$$\mathbf{A}^{(1)}(k, t) = \{n(k, t)\}, \quad (17)$$

and $F_{nn}(k, t)$ immediately can be obtained in a single-exponential form

$$F_{nn}^1(k, t) = G_{nn}^1(k) e^{-d_0(k)t} \equiv S(k) e^{-t/\tau_{nn}(k)}. \quad (18)$$

This analytical expression and the single relaxing mode $d_0(k)$ within the effective single-variable dynamic model $\mathbf{A}^{(1)}$ were surprisingly in very good agreement with the structural relaxation mode, obtained from the five-variable dynamic model $\mathbf{A}^{(5)}$, that is a consequence of negligible thermal relaxation effects in this region of wave numbers. Namely for $k \approx k_{FSDP}$ it was shown in [15, 16], that the relaxation time $\tau_{nn}(k)$ in (18) can be associated with the lifetime of the cages of nearest neighbors in liquid.

Structural relaxation plays very important role in sound propagation in liquids. Namely due to interaction with structural relaxation close to the boundary of hydrodynamic regime, for $k \approx k_{hd}$, the dispersion of longitudinal acoustic excitations $\omega_s(k)$ in liquids shows a bending up towards higher frequencies from the linear hydrodynamic dispersion law, that commonly is known as “positive dispersion” [9]. In Fig. 1 the apparent speed of sound for liquid Ca is shown as a function of wave number. It is seen, that right at $k \approx 0.25$, i.e. close to the boundary of hydrodynamic regime, the apparent speed of sound reaches its maximum that gives evidence of “positive dispersion” in liquid Ca.

The “positive dispersion” strongly depends on density (or pressure) of the system. Recently it was reported a combined experimental and simulation study on supercritical fluids along an isothermal line on phase diagram [17]. The “positive dispersion” showed a strong reduction with decreasing pressure, and in vicinity of the Widom

line the “positive dispersion” for collective excitations almost disappeared. This was an example how some dynamic quantity like “positive dispersion” can discriminate between liquid-like and gas-like fluids.

The “positive dispersion” can be explained within the GCM approach even within the viscoelastic approximation [4], when the coupling with thermal fluctuations is neglected (i.e. $\gamma = 1$). It was shown in [14], that on the boundary of hydrodynamic regime the dispersion law for sound excitations can be obtained within the viscoelastic approximation as

$$\omega_s^{ve}(k) = c_T k \sqrt{1 + \frac{D_L}{d_2^0} k^2 - \frac{D_L^2}{4c_T^2} k^2 + O(k^4)} = c_T k + \beta^{ve} k^3 + \dots, \quad (19)$$

where under the square root there are two contributions proportional to k^2 : the first one is positive and comes from the coupling of acoustic excitations with structural relaxation, and the second contribution is negative and it is the standard renormalization down of the dispersion law due to the damping effects. In Eq. (19) the c_T is the isothermal speed of sound, and d_2^0 from Eq. (14) taken at $\gamma = 1$. The first correction to the linear viscoelastic dispersion law in GCM approach is proportional to the k^3 with the following coefficient:

$$\beta^{ve} \approx c_T \frac{D_L^2}{8} \frac{5 - (c_\infty/c_T)^2}{c_\infty^2 - c_T^2}. \quad (20)$$

The most interesting fact is a possibility for this correction to become even negative for some ratio of the high-frequency and isothermal speeds of sound. Calculations of β^{ve} as a function of density performed in [14] gave evidence that for dense liquids the coefficient β^{ve} is positive and reduces with decreasing density, that was in complete agreement with experimental and simulation findings reported in [17]. The extension of viscoelastic results for β^{ve} on the case of more general thermo-viscoelastic model $\mathbf{A}^{(5)}$ permitted to estimate the role of thermal fluctuations in dispersion of acoustic excitations, that is very important when the system is close to critical point.

Important role of structural relaxation in collective dynamics in liquids is reflected in wave-number dependence of contributions from different hydrodynamic and non-hydrodynamic collective modes to density-density time correlation functions $F_{nn}(k, t)$ or dynamic structure factors $S(k, \omega)$ [18]. Within the GCM approach it is straightforward to represent the GCM expression for the density-density time correlation functions with complex weight coefficients (3) in a form with only real weight coefficients, that directly generalizes the hydrodynamic expression (1). In [16] a general expression for GCM time correlation functions for a system with N_{rel} relaxation processes and N_{pr} pairs of complex-conjugated eigenvalues (propagating modes) was obtained:

$$\frac{F_{nn}^{(N_v)}(k, t)}{S(k)} = \sum_{i=1}^{N_{rel}} A_{nn}^i(k) e^{-d_i(k)t} + \sum_{i=1}^{N_{pr}} [B_{nn}^i(k) \cos(\omega_i(k)t) + D_{nn}^i(k) \sin(\omega_i(k)t)] e^{-\sigma_i(k)t}, \quad (21)$$

where $N_v = N_{rel} + 2N_{pr}$ is the number of dynamic variables in corresponding dynamic model, and all the weight coefficients $A_{nn}^i(k)$, $B_{nn}^i(k)$ and $D_{nn}^i(k)$, that sometimes are called mode strengths [19], are real functions of wave number. Corresponding GCM

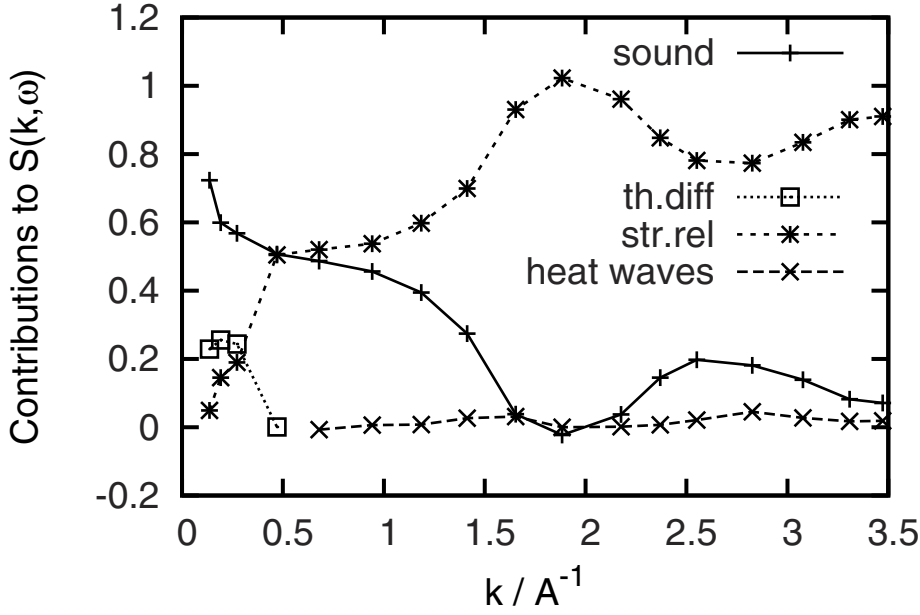


Fig. 3. Strengths of contributions from main hydrodynamic and non-hydrodynamic processes to the density-density time correlation functions for the case of liquid Ca.

expression for dynamic structure factor reads:

$$\frac{S^{(N_v)}(k, \omega)}{S(k)} = \sum_{i=1}^{N_{rel}} A_{nn}^i(k) \frac{2d_i(k)}{\omega^2 + d_i^2(k)} + \sum_{\pm, i=1}^{N_{pr}} \left[B_{nn}^i(k) \frac{\sigma_i(k)}{[\omega \pm \omega_i(k)]^2 + \sigma_i^2(k)} \pm D_{nn}^i(k) \frac{\omega \pm \omega_i(k)}{[\omega \pm \omega_i(k)]^2 + \sigma_i^2(k)} \right]. \quad (22)$$

Now the meaning of weight coefficients is very clear: the coefficients $A_{nn}^i(k)$ reflect the contribution from the i -th relaxing mode to the central peak of dynamic structure factor, while coefficients $B_{nn}^i(k)$ and $D_{nn}^i(k)$ are the strengths of Lorentzian and non-Lorentzian contributions to the side peaks corresponding to the i -th branch of collective excitations. Note, that the non-Lorentzian contributions change the sign right at the frequency $\omega_i(k)$ thus causing the asymmetry of corresponding side peak. The non-Lorentzian contributions are proportional to k in long-wavelength limit, however beyond the hydrodynamic regime they can be quite strong [3].

In Fig. 3 is shown the wave-number dependence of mode strengths from main relaxing and propagating collective modes in liquid Ca, obtained within the dynamic model $\mathbf{A}^{(5)}$. It is seen, that in the long-wavelength limit only the hydrodynamic modes define the shape of dynamic structure factor $S(k, \omega)$. Their mode strengths are in agreement with hydrodynamic results when $k \rightarrow 0$: $A_{nn}^{th} \rightarrow 1 - \gamma^{-1}$, and $B_{nn}^{sound} \rightarrow \gamma^{-1}$. Very important that the ratio of these mode strengths in fact yields the famous Landau-Placzek ratio [1]. The contribution from the hydrodynamic thermodiffusive mode A_{nn}^{th} vanishes quickly beyond the hydrodynamic regime, while the contribution from non-hydrodynamic structural relaxation strongly increases instead. In the region of FSDP of $S(k)$ the structural relaxation completely defines the central peak of $S(k, \omega)$, that is in agreement with analytical results (18). In this region the structural

relaxation is the slowest relaxation process in the liquid, that implies its leading role in de Gennes slowing down of density fluctuations. The Lorentzian contribution from the acoustic excitations strongly decreases beyond the hydrodynamic regime reaching its minimum right at the position of FSDP.

3.2 Shear waves

The simplest extended dynamic model for description of transverse dynamics in pure liquids consists of two dynamic variables:

$$\mathbf{A}^{(2T)} = \{J^T(k, t), \dot{J}^T(k, t)\}, \quad (23)$$

where the extended variable is the first time derivative of the transverse component of mass-current [20]. This dynamic model yields different sets of eigenvalues for wave numbers smaller and larger than

$$k_{sw} = \left[\frac{\rho G(k)}{4\eta(k)} \right]^{\frac{1}{2}} \Big|_{k \rightarrow 0} = \left[\frac{\rho G}{4\eta} \right]^{\frac{1}{2}}, \quad (24)$$

where $G(k)$ and $\eta(k)$ are the wave-number dependent shear modulus and shear viscosity, respectively. For $k < k_{sw}$ one obtains two purely real eigenvalues, that correspond to two relaxing processes:

$$z^+(k) = \frac{G}{\eta} - \frac{\eta}{\rho} k^2, \quad z^-(k) = \frac{\eta}{\rho} k^2. \quad (25)$$

The lowest real eigenvalue is simply the hydrodynamic relaxing mode connected with shear viscosity of the system. Another real eigenvalue corresponds to a transverse non-hydrodynamic relaxing mode and tends in long-wavelength limit to a non-zero constant, defined by the shear modulus and shear viscosity. This eigenvalue decreases with increasing wave number. For $k > k_{sw}$ instead of two relaxing eigenmodes one obtains a complex-conjugated pair of eigenvalues, that correspond to shear waves that can propagate on microscopic scales. Hence, k_{sw} is called the width of propagating gap for shear waves. Shear waves cannot propagate in liquids for $k < k_{sw}$.

The damping and dispersion of shear waves can be estimated from equation

$$z_{sw}^{\pm}(k) = \sigma_{sw}(k) \pm i\omega_{sw}(k) = \frac{\delta(k)}{2} \pm i \left[\frac{k^2 G(k)}{\rho} - \frac{\delta^2(k)}{4} \right]^{\frac{1}{2}}, \quad (26)$$

where

$$\delta(k) = \langle \omega^2 \rangle_{JJ}^T(k) \tau_{JJ}(k),$$

and $\tau_{JJ}(k)$ is the transverse correlation time defined as

$$\tau_{JJ}(k) = \frac{1}{mk_B T} \int_0^{\infty} C^T(k, t) dt,$$

and $\langle \omega^2 \rangle_{JJ}^T(k)$ is the normalized second frequency moment of transverse spectral function

$$\langle \omega^2 \rangle_{JJ}^T(k) = \frac{\int_{-\infty}^{\infty} \omega^2 C^T(k, \omega) d\omega}{\int_{-\infty}^{\infty} C^T(k, \omega) d\omega} \equiv \frac{\langle \dot{J}^T(k) \dot{J}^T(-k) \rangle}{\langle J^T(k) J^T(-k) \rangle}, \quad (27)$$

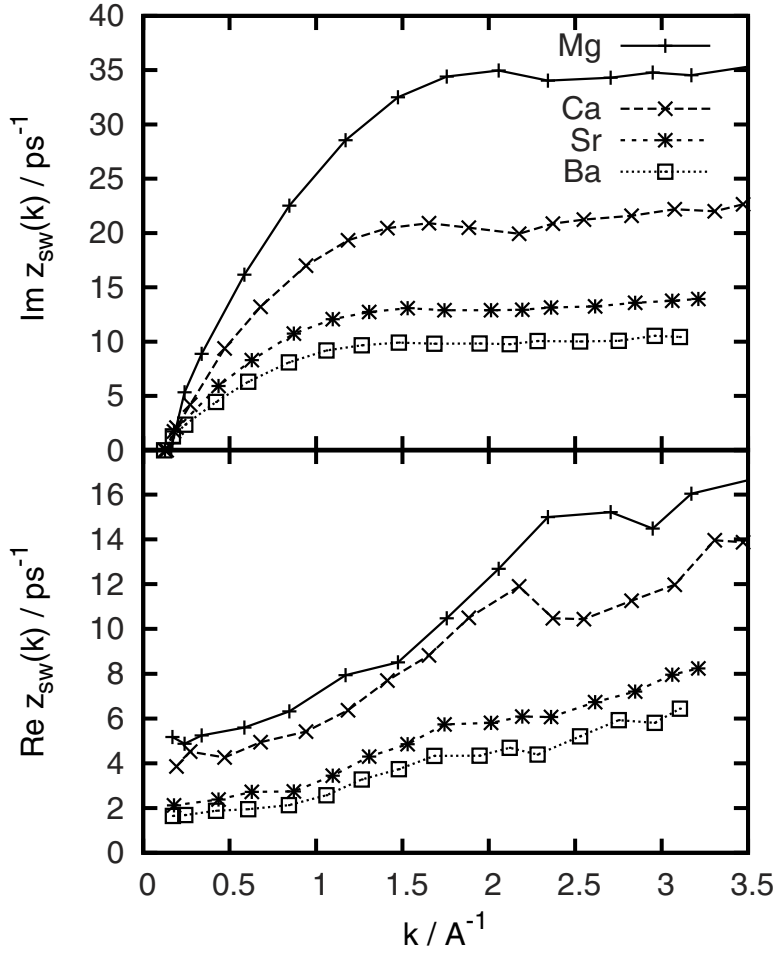


Fig. 4. Dispersion and damping of non-hydrodynamic shear waves for molten Mg, Ca, Sr and Ba at their melting points.

that in the long-wavelength limit is a function of k^2 :

$$\langle \omega^2 \rangle_{JJ}^T(k) = \frac{G(k)}{\rho} k^2. \quad (28)$$

In Fig. 4 the dispersion and damping of shear waves is shown for four alkaline earth liquid metals near corresponding melting points. The propagating gap for shear waves for all four liquid metals is about 0.15 \AA^{-1} . The dispersion of shear waves abruptly increases and around $k \approx 1.8 \text{ \AA}^{-1}$ it reaches the slow short-wavelength asymptote

$$\omega_{sw}(k) \xrightarrow{k \rightarrow \infty} \left[\frac{G(k)}{\rho} \right]^{\frac{1}{2}} k, \quad (29)$$

that in Gaussian regime should be

$$\omega_{sw}(k)|_{k \rightarrow \infty} \sim k^{\frac{1}{2}}.$$

Another tendency in dispersion of shear waves in Fig. 4 is in higher frequencies for lighter particles. The damping of shear waves has a similar tendency: it is larger for systems composed of lighter particles.

3.3 Heat waves

Theoretical description of non-hydrodynamic propagating heat excitations in liquids is quite similar as for the shear waves. A simplest two-variable extended dynamic model [21]

$$\mathbf{A}^{(2h)} = \{h(k, t), \dot{h}(k, t)\} \quad (30)$$

permits to study solutions, that correspond to heat waves in liquids. In (30) the two dynamic variables are the hydrodynamic variable of heat density, and its first time derivative.

Similar as for the shear waves, there exists a propagation gap for heat waves with the width:

$$k_{hw} \simeq \frac{c_V}{2\lambda} \sqrt{\frac{nG^h}{m}}, \quad (31)$$

where G^h is the heat rigidity modulus [21]. For $k < k_{hw}$ one obtains two relaxing eigenmodes

$$z^+(k) = d_3(k) = \frac{c_V G^h}{m\lambda} - \frac{\lambda}{nc_V} k^2$$

$$z^-(k) = d_1(k) = \frac{\lambda}{nc_V} k^2.$$

The lowest eigenvalue is the hydrodynamic heat mode, while the mode $z^+(k)$ corresponds to the non-hydrodynamic relaxing mode $d_3(k)$ obtained within the five-variable dynamic model $\mathbf{A}^{(5)}$ with $\gamma = 1$. For $k > k_{hw}$ one obtains propagating eigenmodes

$$z_{hw}^{\pm}(k) = \frac{\delta(k)}{2} \pm i \left[\frac{\frac{k^2 G^h(k)}{\rho} - \delta^2(k)}{4} \right]^{\frac{1}{2}}, \quad (32)$$

where

$$\delta(k) = \frac{c_V(k)G^h(k)}{m\lambda(k)}.$$

In Fig. 5 the dispersion of heat waves is shown for three liquid metals near their melting points: Mg, Ca and Sr. The width of propagating gap for heat waves is approximately 0.5 \AA^{-1} . Again as for the shear waves the metals with lighter atoms have more high-frequency shear waves.

An interesting issue is the possibility to observe heat waves in the spectrum of density fluctuations from scattering experiments. It is obvious, that the coupling between density and heat fluctuations has to be strong enough in order the heat waves to make some effect on the shape of dynamic structure factors. And this is not the case of liquid metals, where γ is quite close to unity, that means very small coupling between density and heat fluctuations. In Fig. 3 the contributions from heat waves to the dynamic structure factor of liquid Ca is shown by line-connected ‘‘cross’’ symbols. This gives evidence that heat waves in metals cannot be observed in IXS or INS experiments. However, in experiments that measure frequency-dependent specific heat at constant pressure $c_P(\omega)$ one can expect to see some signal from the high-frequency heat waves.

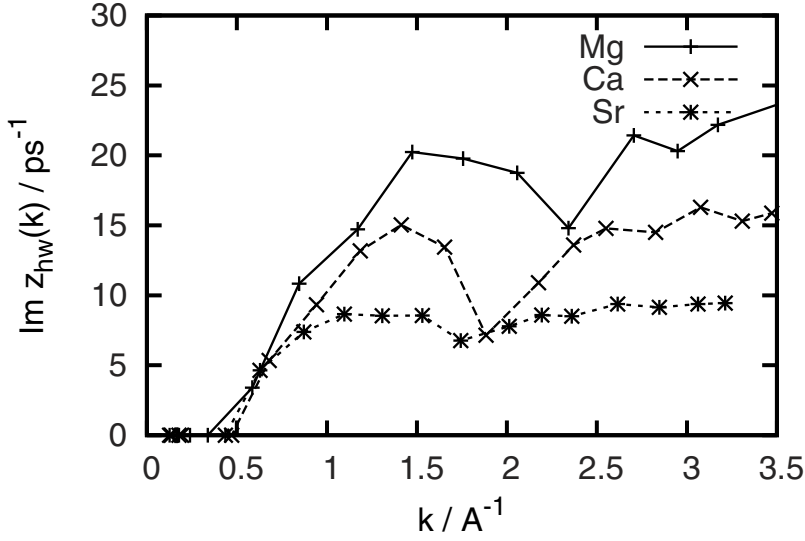


Fig. 5. Dispersion of non-hydrodynamic heat waves for molten Mg, Ca, Sr near their melting points.

3.4 Optic-like excitations in binary liquid alloys

Optic-like phonons in binary crystals are well-defined excitations, that correspond to the motion of nearest neighbors of different kind with opposite phases. Since the optic phonons are the high-frequency excitations in crystals it was believed, that in the case of liquids the optic-like excitations cannot exist. However, it was shown in [23], that calculated in molecular dynamic simulations transverse concentration current autocorrelation functions contained damped high-frequency oscillations, that implied existence of transverse optic-like modes.

A simplest theory of optic-like excitations was constructed firstly for the transverse case within the two-variable dynamic model [23]:

$$\mathbf{A}^{(2xT)} = \{J_x^T(k, t), \dot{J}_x^T(k, t)\}, \quad (33)$$

where $J_x^T(k, t)$ is the spatial Fourier components of the density of mass-concentration current

$$\mathbf{J}_x(\mathbf{r}, t) = \frac{m_1 x_2}{\sqrt{N}} \sum_{i=1}^{N_1} \mathbf{v}_{1,i}(t) \delta(\mathbf{r} - \mathbf{r}_{1,i}(t)) - \frac{m_2 x_1}{\sqrt{N}} \sum_{i=1}^{N_2} \mathbf{v}_{2,i}(t) \delta(\mathbf{r} - \mathbf{r}_{2,i}(t)),$$

that describes the motion of different species with opposite phases. Note that $J_x^T(k, t)$ does not correspond to fluctuations of conserved quantities. The second dynamic variable in (33) is the first time derivative of $J_x^T(k, t)$.

Two eigenmodes obtained for the dynamic model $\mathbf{A}^{(2xT)}$ read:

$$z_{xT}^{\pm} = \frac{\langle \omega^2 \rangle_{xx}^T \tau_{xx}^T}{2} \pm \frac{\sqrt{(\langle \omega^2 \rangle_{xx}^T \tau_{xx}^T)^2 - 4 \langle \omega^2 \rangle_{xx}^T}}{2}, \quad (34)$$

where

$$\langle \omega^2 \rangle_{xx}^T(k) = \frac{\langle \dot{J}_x^T(k) \dot{J}_x^T(-k) \rangle}{\bar{m} x_1 x_2 k_B T}$$

it the normalized second frequency moment of the spectral function of transverse mass-current, and

$$\tau_{xx}^T(k) = \frac{1}{\bar{m}x_1x_2k_B T} \int_0^\infty C_{xx}^T(k, t) dt$$

is the correlation time associated with corresponding time correlation function. Note, that for $k = 0$ there exists an equality

$$D_{12} = \frac{1}{\bar{m}S_{xx}(0)} \int_0^\infty C_{xx}^T(k, t) dt, \quad (35)$$

where D_{12} is the mutual diffusivity, and $S_{xx}(0)$ is the mass-concentration static structure factor at $k = 0$ [22].

The condition for existence of transverse optic-like modes in liquid alloys follows from Eq. 34, because for a pair of complex-conjugated solutions one needs the expression under square root to be negative. Hence, it was obtained, that the condition of existence of transverse optic modes is [23]:

$$\delta_x = \frac{\langle \omega^2 \rangle_{xx}^T(0) \bar{m}^2 D_{12}^2 S_{xx}^2(0)}{4(x_1x_2k_B T)^2} < 1, \quad (36)$$

that holds for binary liquid alloys with low mutual diffusivity and without some tendency to demixing in the alloy. Similarly, the damping of transverse optic-like excitations in the long-wavelength region is as follows:

$$\sigma_x^T(k \rightarrow 0) = \frac{\langle \omega^2 \rangle_{xx}^T(0) D_{12} S_{xx}(0)}{2x_1x_2k_B T}, \quad (37)$$

and dispersion reads:

$$\omega_x^T(k \rightarrow 0) = \sqrt{\langle \omega^2 \rangle_{xx}^T(0) - \sigma^2(0)}. \quad (38)$$

Analysis of damping of transverse optic-like modes permits to conclude: the more high-frequency excitation the higher is its damping; high mutual diffusivity and tendency to demixing when the particles tends to be surrounded by the like-particles do not favor for existence of optic modes.

Theory of longitudinal optic-like excitations was reported in Ref. [24]. For the case of longitudinal dynamics one has to consider a three-variable dynamic model:

$$\mathbf{A}^{(3x)} = \{n_x(k, t), J_x^L(k, t), \dot{J}_x^L(k, t)\}, \quad (39)$$

where

$$n_x(k, t) = \frac{1}{\bar{m}} \{m_1x_2n_1(k, t) - m_2x_1n_2(k, t)\} \quad (40)$$

is the hydrodynamic variable of mass-concentration density [22]. Here

$$n_\alpha(k, t) = \frac{1}{\sqrt{N}} \sum_{i=1}^{N_\alpha} e^{i\mathbf{k}\mathbf{r}_{\alpha,i}(t)}, \quad \alpha = 1, 2,$$

are the partial densities. The mass-concentration density is connected with the longitudinal component of mass-concentration current via continuity equation, as it should be:

$$\frac{\partial n_x}{\partial t} = \frac{ik}{\bar{m}} J_x^L(k, t). \quad (41)$$

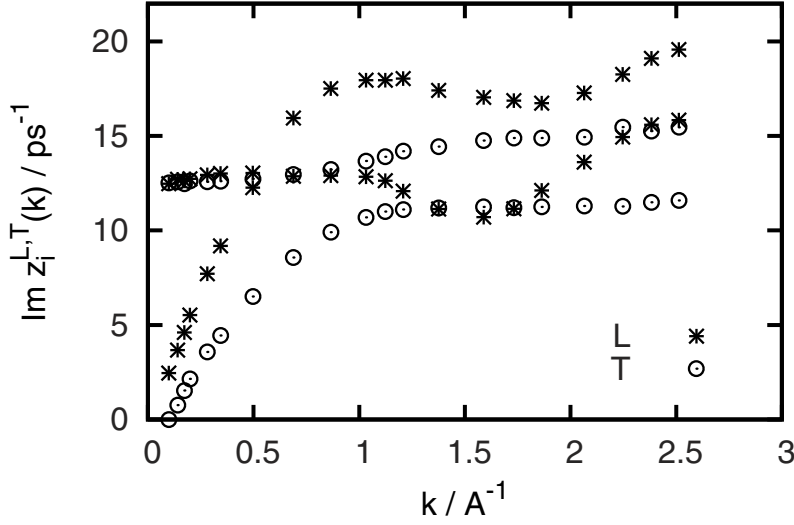


Fig. 6. Dispersion of longitudinal (symbols “star”) and transverse (symbol “circle”) collective excitations in a liquid alloy $\text{Na}_{0.4}\text{K}_{0.6}$ at temperature 373 K.

The third dynamic variable in the set $\mathbf{A}^{(3x)}$ is the first time derivative of longitudinal mass-current. In the long-wavelength region one obtains three eigenvalues. One of them is purely real and corresponds to hydrodynamic relaxing process connected with mutual diffusivity:

$$d_c(k) = D_{12}k^2, \quad (42)$$

while two other eigenvalues are

$$z_x^\pm(k \rightarrow 0) = \sigma(k) \pm \sqrt{\sigma^2(k) - \langle \omega^2 \rangle_{xx}(k)}, \quad \sigma(k) = \frac{\langle \omega^2 \rangle_{xx}(k)}{2\tau_{xx}(k)\langle \omega^2 \rangle_{xx}(k)}, \quad (43)$$

that in the long-wavelength limit yields almost identical condition for existence of longitudinal optic modes as in the transverse case:

$$\delta_x = \frac{\langle \omega^2 \rangle_{xx}(0)D_{12}^2 S_{xx}^2(0)\bar{m}^2}{4(x_1 x_2 k_B T)^2} < 1 \quad (44)$$

It is remarkable, that the two different dynamic models: one is three-variable model for longitudinal case, and the second is two-variable model for transverse dynamic - result in consistent expressions for damping of optic modes in the long-wavelength limit. The only difference is in the second frequency moments of corresponding spectral functions, which for the case of non-ionic melts, i.e. systems with short-range interactions only, must be identical in the long-wavelength limit due to symmetry reasons.

In Fig. 6 longitudinal and transverse branches of collective excitations are shown for a liquid alloy $\text{Na}_{0.4}\text{K}_{0.6}$ at temperature 373 K. It is seen, that the optic-like branches are well-defined in the long-wavelength region, and longitudinal optic modes have the same frequency as the transverse optic modes.

3.5 Does the “fast sound” exist in disparate mass binary liquid alloys?

Binary liquid alloys with disparate masses are of special interest because of reported observations in INS experiments [25] and molecular dynamics simulations [26] of so

called “fast sound”. The “fast sound” excitations were observed for the first time in molecular dynamics simulations of a molten alloy Li_4Pb in the shape of calculated partial dynamic structure factors $S_{\text{LiLi}}(k, \omega)$. This partial dynamic structure factor of the light component revealed down to the smallest accessible wavenumbers a high-frequency side peak that was ascribed to a collective mode propagating via the light component of the molten alloy.

Neutron scattering experiments on molten alloys Li_4Pb and Li_4Tl supported the simulations results on existing high-frequency propagating modes of “fast sound”. Similar behaviour of the high-frequency collective modes was observed in gas mixtures He-Xe [27], He-Ne [28] and He-Ar [29], although there were no indications how the high-frequency branch of collective excitations would behave in the limit $k \rightarrow 0$.

One of the deficiencies of the standard schemes of estimation of dispersion of collective modes via side peak locations of the partial dynamic structure factors is in complete neglect of cross-correlations between species in the binary liquid alloys. It was shown in Ref. [23], that the cross-correlations between partial quantities is negligible for large wave numbers, while in the long-wavelength region they are very strong and cannot be neglected. Completely different wave-number dependence have the cross-correlations between quantities that correspond to total density and concentration density fluctuations: they are negligible in the long-wavelength region and become quite strong for large wave numbers [23]. Hence a correct numerical way of estimation of dispersion of collective excitations in disparate mass liquid alloys must be based on analysis of peak positions of four different current spectral functions: two partial spectral functions $C_{ii}(k, \omega)$, $i = A, B$ and two spectral functions $C_{ii}(k, \omega)$, $i = t, x$, that reflect total- and mass-concentration-current autocorrelations.

However, only a theoretical analysis that accounts for all possible cross-correlations can predict correct dispersion curves for non-hydrodynamic propagating processes and shed light on the origin of observed “fast sound”. The GCM analysis was first applied to analysis of transverse dynamics in Li_4Pb in Ref. [23]. Later on a complete study of generalized thermodynamic quantities, transport coefficients and longitudinal collective modes in Li_4Pb was performed in Ref. [30]. Analysis of analytical expression for damping of the high-frequency non-hydrodynamic excitations as a function of mass ratio in binary liquids were reported in [31]. In that study it was for the first time shown, that for Li_4Pb there exists a crossover in contributions from propagating modes to the partial dynamic structure factor of light component $S_{\text{LiLi}}(k, \omega)$, that caused an impression of almost linear dispersion of “fast sound”.

Recently a molecular dynamics study and GCM analysis of collective dynamics were reported for Li_4Tl liquid alloy [32]. The dispersion of different branches of longitudinal and transverse collective excitations obtained within the GCM approach is shown in the top frame of Fig. 7. For comparison a dispersion, obtained from peak positions of the partial current spectral function $C_{\text{LiLi}}^L(k, \omega)$ is shown by line-connected open boxes. It is seen, that agreement between GCM eigenvalues and peak positions is very good for $k > 0.7 \text{ \AA}^{-1}$. For smaller wave numbers the dispersion obtained from peak positions of partial spectral function $C_{\text{LiLi}}^L(k, \omega)$ is shifting towards lower frequencies. At $k \approx 0.2 \text{ \AA}^{-1}$ there is even a situation with two peaks in the frequency dependence of $C_{\text{LiLi}}^L(k, \omega)$, while for smaller wave numbers the peaks of $C_{\text{LiLi}}^L(k, \omega)$ are in good agreement with hydrodynamic dispersion law shown by long-dashed line in the top frame. In order to understand such a specific behavior of dispersion, obtained from peak positions of $C_{\text{LiLi}}^L(k, \omega)$, in the bottom frame of Fig. 7 are shown leading contributions to the partial dynamic structure factor of light component $S_{\text{LiLi}}(k, \omega)$ in Li_4Tl . One can see, that in the long-wavelength region there is a crossover in contributions from the high- and low-frequency branches. In fact,

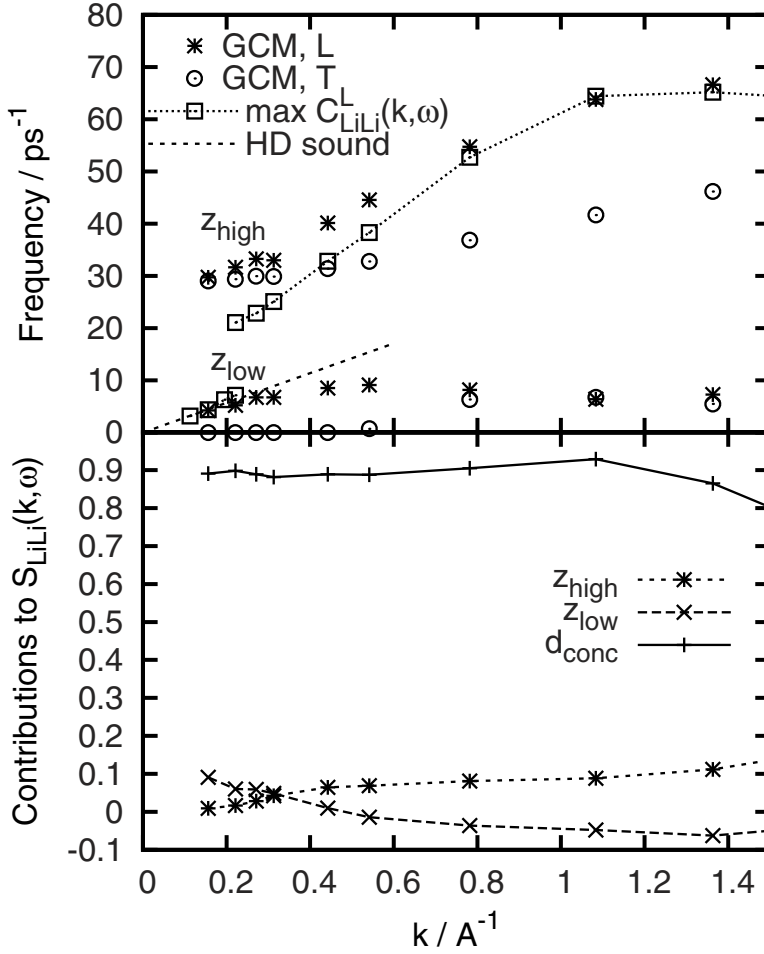


Fig. 7. Dispersion of longitudinal and transverse collective excitations in a liquid alloy Li_4Tl at temperature 753 K (top frame) and contributions from collective excitations and relaxing concentration mode to the partial dynamic structure of light component $S(k, \omega)$ (bottom frame). By line-connected open boxes are shown peak positions of longitudinal partial current spectral function $C_{\text{LiLi}}^L(k, \omega)$. Long-dashed line corresponds to hydrodynamic sound dispersion with speed of propagation 2845 m/s.

the side peak of $S_{\text{LiLi}}(k, \omega)$ for $k > 0.4 \text{\AA}^{-1}$ mainly corresponds to the high-frequency branch, shifted a little by a negative contribution from the low-frequency branch. However, in the long-wavelength limit the contribution from non-hydrodynamic high-frequency branch vanishes and the side peak of $S_{\text{LiLi}}(k, \omega)$ corresponds to only the low-frequency branch. This explains the behaviour of numerical dispersion (open boxes in Fig. 7) and other numerical reports of a merger of the high- and low-frequency branches into a single hydrodynamic dispersion law [33, 34].

In summary, the GCM analysis of collective dynamics in disparate mass liquid alloys permits to estimate the correct dispersion of the high- and low-frequency branches of collective excitations. The real high-frequency excitations of mainly propagating partial densities of light atoms makes sense only for $k > 0.7 \text{\AA}^{-1}$. For smaller wavenumbers the dispersion of high-frequency branch tends to a finite

non-zero frequency. A merger of the high- and low-frequency branches into the linear hydrodynamic dispersion law, that was reported to occur close to the boundary of hydrodynamic regime [33,34] is in fact an unreal effect because of crossover in contributions from the high- and low-frequency branches to the partial spectral function of light component.

4 Conclusions and new challenges for the theory of non-hydrodynamic processes

In this small review main results for non-hydrodynamic collective modes in liquid metals and alloys were presented. The studies performed in combination of MD simulations and theoretical GCM approach permit to extract from the MD-derived time correlation functions the spectrum of collective excitations, including the non-hydrodynamic collective excitations, wavenumber dependence of non-propagating relaxation processes, as well as their contributions to the shape of the studied time correlation functions and corresponding spectral functions.

The GCM approach proved over the last fifteen years its ability to describe correctly non-hydrodynamic processes in liquids. However some new scattering experiments and simulations of liquid and glass systems yield new challenges for the GCM approach, that can be listed as follows:

- i) description of low-frequency collective modes that form the excess of vibrational density of states known as Boson peak in metallic glasses;
- ii) *ab initio* simulations permit to obtain information on adiabatic redistribution of the valence electron density due to ionic motion. One of the challenges is to extend the GCM approach in order to take into account explicitly effects of electron density polarization on collective excitations in liquid metals. There exists a theory of liquid metals as a two-component electron-ion liquid [35], that perhaps can be used for extension of the GCM approach;
- iii) for liquid systems with covalent bonds the existence of short-time units like dimers, small clusters or rings essentially affects the shape of density-density time correlation functions. Therefore an extension of the GCM scheme towards accounting the existence of molecular-like units with rather short lifetime is needed.

References

1. J.-P. Boon, S. Yip, *Molecular Hydrodynamics* (McGraw-Hill, 1980)
2. J.-P. Hansen, I.R. McDonald, *Theory of Simple Liquids* (Academic, 1986)
3. C. Cohen, J.W.H. Sutherland, J.M. Deutch, *Phys. Chem. Liq.* **2**, 213 (1971)
4. U. Balucani, M. Zoppi, *Dynamics of the liquid state* (Clarendon, 1994)
5. I.M. deSchepper, E.G.D. Cohen, C. Bruin, J.C. van Rijs, W. Montfrooij, L.A. de Graaf, *Phys. Rev. A* **38**, 271 (1988)
6. I. Mryglod, *Condens. Matter Phys.* **1**, 753 (1998)
7. I.M. Mryglod, I.P. Omelyan, M.V. Tokarchuk, *Mol. Phys.* **84**, 235 (1995)
8. T. Bryk, I. Mryglod, G. Kahl, *Phys. Rev. E* **56**, 2903 (1997)
9. T. Scopigno, G. Ruocco, F. Sette, *Rev. Mod. Phys.* **77**, 881 (2005)
10. T. Bryk, I. Mryglod, *Condens. Matter Phys.* **7**, 471 (2004)
11. D.D. Joseph, L. Preziosi, *Rev. Mod. Phys.* **61**, 41 (1989)
12. F. Bencivenga, A. Cunsolo, M. Krisch, G. Monaco, G. Ruocco, F. Sette, *Europhys. Lett.* **75**, 70 (2006)
13. J.-F. Wax, R. Albaki, J.-L. Bretonnet, *Phys. Rev. B* **62**, 14818 (2000)

14. T. Bryk, I. Mryglod, T. Scopigno, G. Ruocco, F. Gorelli, M. Santoro, J. Chem. Phys. **133**, 024502 (2010)
15. T. Bryk, I. Mryglod, Phys. Rev. E **64**, 322021 (2001)
16. T. Bryk, I. Mryglod, J. Phys.: Condens. Matter. **13**, 1343 (2001)
17. G.G. Simeoni, T. Bryk, F.A. Gorelli, M. Krisch, G. Ruocco, M. Santoro, T. Scopigno, Nature Phys. **6**, 503 (2010)
18. T. Bryk, I. Mryglod, Condens. Matter Phys. **11**, 139 (2008)
19. N.H. March, M.P. Tosi, *Coulomb Liquids* (Academic Press, 1984)
20. T. Bryk, I. Mryglod, Phys. Rev. E **62**, 2188 (2000)
21. T. Bryk, I. Mryglod, Phys. Rev. E **63**, 051202 (2001)
22. A.B. Bhatia, D.E. Thornton, N.H. March, Phys. Chem. Liq. **4**, 97 (1974)
23. T. Bryk, I. Mryglod, J. Phys.: Condens. Matter. **12**, 6063 (2000)
24. T. Bryk, I. Mryglod, J. Phys.: Condens. Matter. **14**, L445 (2002)
25. P.H.K. de Jong, P. Verkerk, C.F. de Vroege, L.A. de Graaf, W.S. Howells, S.M. Bennington, J. Phys.: Condens. Matter. **6**, L681 (1994)
26. J. Bosse, G. Jacucci, M. Ronchetti, W. Schirmacher, Phys. Rev. Lett. **57**, 3277 (1986)
27. A. Campa, E.G.D. Cohen, Phys. Rev. Lett. **61**, 853 (1988)
28. W. Montfrooij, P. Westerhuijs, V.O. de Haan, I.M. de Schepper, Phys. Rev. Lett. **63**, 544 (1989)
29. H.E. Smorenburg, R.M. Crevecoeur, I.M. de Schepper, Phys. Lett. A **211**, 118 (1996)
30. T. Bryk, I. Mryglod, Condens. Matter Phys. **7**, 285 (2004)
31. T. Bryk, I. Mryglod, J. Phys.: Condens. Matter. **17**, 413 (2005)
32. T. Bryk, J.-F. Wax, Phys. Rev. B **80**, 184206 (2009)
33. R. Fernandez-Perea, M. Alvarez, F.J. Bermejo, P. Verkerk, B. Roessli, E. Enciso, Phys. Rev. E **58**, 4568 (1998)
34. E. Enciso, N.G. Almarza, P. Dominguez, M.A. Gonzalez, F.J. Bermejo, Phys. Rev. Lett. **74**, 4233 (1995)
35. N.H. March, M.P. Tosi, Ann. Phys. **81**, 414 (1973)